Eur. Phys. J. B **42**, 477–482 (2004)
DOI: 10.1140/epjb/e2005-00005-y

THE EUROPEAN PHYSICAL JOURNAL B

The optimum elastic wave band gaps in three dimensional phononic crystals with local resonance

Xin Zhang[1,2,a], Zhengyou Liu[1,3,4], and Youyan Liu[4]

[1] Department of Physics, Wuhan University, 430072 Wuhan, P.R. China
[2] Department of Applied Physics, Guangdong University of Technology, 510090 Guangzhou, P.R. China
[3] PBG Research Center, National University of Defense Technology, 410072 Changsha, P.R. China
[4] Department of Applied Physics, South China University of Technology, 510640 Guangzhou, P.R. China

Received 31 March 2004 / Received in final form 16 August 2004
Published online 18 January 2005 –

Abstract. Using multiple-scattering theory, we investigate the optimization of the elastic wave band gaps of three dimensional three-component phononic crystals with local resonance. The optimum gaps of two systems including Au spheres coated with Pb embedded in Si matrix and Pb spheres coated with plastic embedded in Si matrix are obtained by tuning the ratio of the inner and the outer radii of the coating layers. It also shows that the elastic wave band gaps for the two systems versus the filling fractions and the radius ratio display different features.

PACS. 43.20.+g General linear acoustics – 43.35.+d Ultrasonics, quantum acoustics, and physical effects of sound – 43.40.+s Structural acoustics and vibration

1 Introduction

In recent years, there has been growing interest in classical wave propagation in periodic composite media. The study of photonic crystals has led the way, with the theoretical prediction and experimental realization of photonic band gaps [1,2]. Recently, a great deal of attention has extended to the phononic crystals, the counterpart of photonic crystals, for which elastic waves (EL) and/or acoustic waves (AC) are concerned [3–30]. As in the photonic crystals, the basis of the whole applications of phononic crystals, such as acoustic/elastic wave filters depends on the existence of wide frequency band gaps in which sound and vibration are forbidden. In addition, the study of the EL and AC waves will provide richer physics because of their vector character.

In the previous works, the study of phononic crystals is mainly focused on the two-component systems and the complete band gaps are mainly due to Bragg scattering and the lattice structure, the mass density contrast and the wave velocity contrast of the two components play important roles [3–9,17–29]. It is also realized that the resonance of the structural unit in two component phononic crystal is important in opening the bandgaps [10–16,30]. Recently, a recipe for guaranteeing the existence of elastic wave bandgap was proposed. It requires the introduction of locally resonant structural units, formed with heavy hard cores with soft coatings embedded in the matrices [10,12]. It has also been found that the elastic wave band gap properties can be tuned continuously from a resonance gap to a Bragg gap just by varying the elastic properties of the coating layer [12]. The transmission property of an elastic wave in three-component systems is also investigated experimentally and theoretically [30].

In this article, we optimize the bandgap of the three dimensional (3D) three-component phononic crystals with local resonance. We consider two kinds of system in which the gap widths exhibit respectively two different behaviors with increasing the filling fraction [12]. One is formed with Au spheres coated by Pb embedded in Si matrix, the other consists of a Pb sphere coated by plastic, embedded in Si matrix. They both fulfill the recipe that the coating layer is soft relative to the core and matrix which guarantees the resonance band gap formation, but according to reference [12], the two systems have different behavior in gap opening. Their complete band gaps are systemically optimized by modulating the thickness of the coating layer, resulting in the optimum gaps. All the calculations are performed using the multiple-scattering method. We outline the multiple-scattering theory in Section 2. Section 3 presents the results and discussions and Section 4 gives a summary of this article.

2 Method

Multiple scattering of elastic waves by particles has been extensively studied in the last 20 years. In this section we

[a] e-mail: phxzhang@scut.edu.cn

outline the multiple-scattering theory (MST) for elastic waves [11,12].

In a homogeneous medium, the elastic wave equation may be written as

$$(\lambda+2\mu)\nabla(\nabla\cdot\mathbf{u})-\mu\nabla\times\nabla\times\mathbf{u}=-\rho\omega^2\mathbf{u}, \quad (1)$$

where ρ is the density and λ, μ are the Lamé constants of the medium. Now, we consider a composite medium that contains a host matrix and embedded coating scatterers. The incident wave for scatterer i may be expressed as

$$u^{in}(\mathbf{r}_i)=\sum_{lm\sigma}a^i_{lm\sigma}\mathbf{J}_{lm\sigma}(\mathbf{r}_i), \quad (2)$$

and the scattered wave by scatter i may be expressed as

$$u^{sc}(\mathbf{r}_i)=\sum_{lm\sigma}b^i_{lm\sigma}\mathbf{H}_{lm\sigma}(\mathbf{r}_i), \quad (3)$$

where, r_i is measured from the center of scatterer i, $\mathbf{J}_{lm\sigma}(r)$ and $\mathbf{H}_{lm\sigma}(r)$ are defined as

$$\begin{aligned}\mathbf{J}_{lm1}(\mathbf{r})&=\frac{1}{\alpha}\nabla[j_l(\alpha r)Y_{lm}(\hat{\mathbf{r}})],\\ \mathbf{J}_{lm2}(\mathbf{r})&=\nabla\times[rj_l(\beta r)Y_{lm}(\hat{\mathbf{r}})],\\ \mathbf{J}_{lm3}(\mathbf{r})&=\frac{1}{\beta}\nabla\times\nabla\times[rj_l(\beta r)Y_{lm}(\hat{\mathbf{r}})],\end{aligned} \quad (4)$$

and

$$\begin{aligned}\mathbf{H}_{lm1}(\mathbf{r})&=\frac{1}{\alpha}\nabla\times[h_l(\alpha r)Y_{lm}(\hat{\mathbf{r}})],\\ \mathbf{H}_{lm2}(\mathbf{r})&=\nabla\times[rh_l(\beta r)Y_{lm}(\hat{\mathbf{r}})],\\ \mathbf{H}_{lm3}(\mathbf{r})&=\frac{1}{\beta}\nabla\times\nabla\times[rh_l(\beta r)Y_{lm}(\hat{\mathbf{r}})],\end{aligned} \quad (5)$$

where $\alpha=\omega\sqrt{\rho/(\lambda+2\mu)}$, $\beta=\omega\sqrt{\rho/\mu}$, $j_l(x)$ is the spherical Bessel function, $h_l(x)$ is the spherical Hankel function of the first kind. The index σ ranging from 1 to 3 stands for three kinds of modes: σ=1 is for the longitudinal mode, and $\sigma=2$, 3 represent the two transverse modes. According to multiple-scattering theory, the wave incident on a given scatterer consists of two parts, one is the externally incident wave, $\mathbf{u}^{in(0)}(\mathbf{r}_i)$, which may be expressed as

$$\mathbf{u}^{in(0)}(\mathbf{r}_i)=\sum_{lm\sigma}a^{i(0)}_{lm\sigma}\mathbf{J}_{lm\sigma}(\mathbf{r}_i). \quad (6)$$

The second part is the sum of all the scattered waves except that from scatterer i, given by

$$\mathbf{u}^{in}(\mathbf{r}_i)-\mathbf{u}^{in(0)}(\mathbf{r}_i)=\sum_{j\neq i}\sum_{l''m''\sigma''}b^j_{l''m''\sigma''}\mathbf{H}_{l''m''\sigma''}(\mathbf{r}_j), \quad (7)$$

where r_i and r_j refer to the position of the same spatial point measured from scatterer i and j respectively. With $\mathbf{R}_{i(j)}$ denoting the position of scatterer $i(j)$, we have $\mathbf{r}_j=\mathbf{r}_i+\mathbf{R}_i-\mathbf{R}_j$. It may be proved that

$$\mathbf{H}_{l''m''\sigma''}(\mathbf{r}_i+\mathbf{R}_i-\mathbf{R}_j)=\sum_{lm\sigma}G_{l''m''\sigma''lm\sigma}(\mathbf{R}_i-\mathbf{R}_j)\mathbf{J}_{lm\sigma}(\mathbf{r}_i), \quad (8)$$

where G is the vector structure constant, given by

$$G_{lm\sigma l'm'\sigma'}(\mathbf{R})=\begin{cases}X^{\alpha}_{lml'm'}(\mathbf{R}), & \sigma=\sigma'=1\\ \sum_{\mu}c(l1lm-\mu\mu)\mathrm{X}^{\beta}_{lm-\mu l'm'-\mu'}(\mathbf{R})c(l'1l'm'-\mu\mu), & \sigma=\sigma'=2,\ 3\\ -i\left(\frac{2l'+1}{l'+1}\right)^{1/2}\sum_{\mu}c(l1lm-\mu\mu) & \\ \quad\times X^{\beta}_{lm-\mu l'-1m'-\mu'}(\mathbf{R})c(l'-11l'm'-\mu\mu), & \sigma\neq\sigma';\ \sigma,\ \sigma'\neq 1,\end{cases} \quad (9)$$

$X^{\kappa}_{lml'm'}(R)$ is the structure constant for scalar waves, defined as

$$\mathrm{X}^{\kappa}_{lml'm'}(\mathbf{R})=4\pi\sum_{l''}i^{l'+l''-l}C^{lm}_{l'm'l''m-m'}h_{l''}(\kappa R)Y_{l''m-m'}(\hat{\mathbf{R}}). \quad (10)$$

Here $C^{lm}_{l'm'l''m''}$ is an integral,

$$C^{lm}_{l'm'l''m''}=\iint_s Y_{lm}(\Omega)Y^*_{l'm'}(\Omega)Y^*_{l''m''}(\Omega)d\Omega. \quad (11)$$

By defining $G^{ij}_{l''m''\sigma''lm\sigma}=G_{l''m''\sigma''lm\sigma}(\mathbf{R}_i-\mathbf{R}_j)$, $\mathbf{H}_{l''m''\sigma''}(\mathbf{r}_j)$ may be expressed as

$$\mathbf{H}_{l''m''\sigma''}(\mathbf{r}_j)=\sum_{lm\sigma}G^{ij}_{l''m''\sigma''lm\sigma}\mathbf{J}_{lm\sigma}(\mathbf{r}_i). \quad (12)$$

For a given scatterer, the scattered displacement field is completely determined from the incident field through the scattering matrix. There is a deterministic relation between the expansion coefficients $A=\{a^j_{lm\sigma}\}$ and $\mathbf{B}=\{\mathbf{b}^j_{lm\sigma}\}$:

$$b^j_{l''m''\sigma''}=\sum_{l'm'\sigma'}t^j_{l''m''\sigma''l'm'\sigma'}a^j_{l'm'\sigma'}, \quad (13)$$

$$B=TA,$$

where the scattering matrix $T=\{t_{lm\sigma l'm'\sigma'}\}$ can be obtained from the elastic Mie scattering solution of a scatter. Here the scatterer is a coated sphere and thus requires the boundary conditions with displacement and normal stress continuity at the interface of all the layers. Substituting equations (2), (6), (12) and (13) into equation (7), we arrive at

$$\sum_{jl'm'\sigma'}\left[\delta_{ij}\delta_{ll'}\delta_{mm'}\delta_{\sigma\sigma'}-\sum_{l''m''\sigma''}t^j_{l''m''\sigma''l'm'\sigma'}G^{ij}_{l''m''\sigma''lm\sigma}\right]a^j_{l'm'\sigma'}=a^{i(0)}_{lm\sigma}. \quad (14)$$

This is the final equation for a multiple-scattering system. For a finite and/or disordered system, we must solve this equation in order to investigate the system response to external perturbations. The normal modes of the system may be obtained by solving the following secular equation, in the absence of an external incident wave:

$$\det \left| \delta_{ij}\delta_{ll'}\delta_{mm'}\delta_{\sigma\sigma'} - \sum_{l''m''\sigma''} t^{j}_{l''m''\sigma''l'm'\sigma'} G^{ij}_{l''m''\sigma''lm\sigma} \right| = 0. \quad (15)$$

For a periodic system, equation (15) may be transformed to

$$\det \left| \delta_{ss'}\delta_{ll'}\delta_{mm'}\delta_{\sigma\sigma'} - \sum_{l''m''\sigma''} t^{s'}_{l''m''\sigma''l'm'\sigma'} G^{ss'}_{l''m''\sigma''lm\sigma}(\mathbf{k}) \right| = 0, \quad (16)$$

where s and s' label the scatterers in the unit cell with position vector $\mathbf{o}_s$ and $\mathbf{o}_{s'}$, and $G^{ss'}_{l''m''\sigma''lm\sigma}(\mathbf{k})$ is defined as

$$G^{ss'}_{l''m''\sigma''lm\sigma}(\mathbf{k}) = \sum_{\mathbf{R}} G_{l''m''\sigma''lm\sigma}(\mathbf{o}_s - \mathbf{o}_{s'} - \mathbf{R}) \exp(i\mathbf{k}\cdot\mathbf{R}), \quad (17)$$

where the sum $\sum_{\mathbf{R}}$ is over all lattice sites. The solution of equation (16) gives the band structure of an elastic periodic system.

3 Results and discussions

We first consider the composite system with Au spheres coated by Pb embedded in the Si background. The physical parameters of the three components satisfy the requirement that the coating layer should be softer than both the matrix and core (the part to be coated) in order to form the local resonance structure. For this system, it is known that the resonance bandgap experiences the following variation with increasing filling fraction: the gap width increases first, reaches a maximum at a medium filling fraction, then starts to decrease before finally disappearing [12]. This can be explained as follows: at low and mediate filling fraction, the resonant mechanism remains dominant, but with the filling fraction further increasing, the coupling between the neighboring local resonant units gets more and more prominent, the local resonance of each unit finally evolves into the collective motions of the whole system, the local resonances are not "local" any longer, the bandgap finally closes up [12]. The material parameters are chosen as follows: $\rho = 19.5$ g/cm^3, $C_l = 3.36$ km/s, $C_t = 1.24$ km/s for Au; $\rho = 11.4$ g/cm^3, $C_l = 2.16$ km/s, $C_t = 0.86$ km/s for Pb; $\rho = 2.33$ g/cm^3, $C_l = 8.95$ km/s, $C_t = 5.36$ km/s for Si; where ρ, C_l and C_t are, respectively, the density, the longitudinal and transverse sound velocity. We arrange the coated spheres in a fcc structure of filling fraction (core + coating layer) 0.204, and employ the ratio of the inner and the outer radii of the coating, i.e., r_{in}/r_{out} as a tuning parameter. When it is 12/23, we get the elastic wave band structure as shown in Figure 1. A sizable absolute gap is seen at frequency 0.48, in units of $d/2\pi C_t$, where C_t is the transverse velocity in a Si matrix and d is the diameter of the coated sphere. This gap is owing to the local resonances of the coated sphere and it has also been proved to be independent of the arrangement of the spheres [12]. The fairly flat band defines the low edge of this gap.

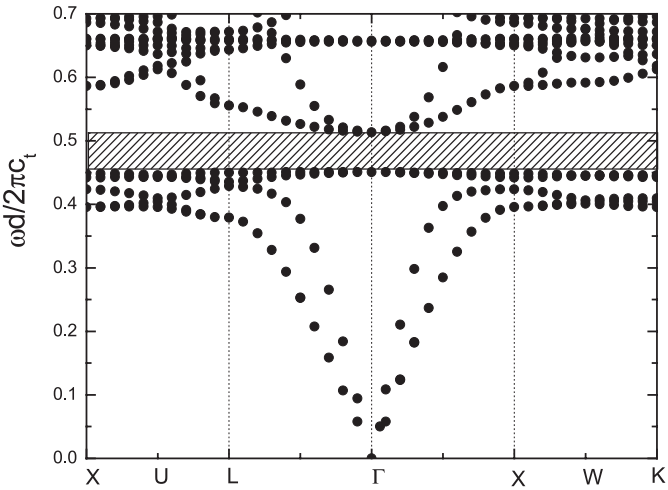

Fig. 1. The elastic wave band structure of Au spheres coated by Pb embedded in Si matrix arranged in a fcc structure. The gap is marked by the shaded area. The filling fraction of the coated spheres is 0.204 and the radius ratio r_{in}/r_{out} is 12/23.

The essential physics in the bandgap formation of the three component phononic crystal with the locally resonant unit can be captured through a "spring model": in each local unit, the inner core serves as a heavy mass and the coating layer serves as a soft spring, thus each local unit acts as a simple oscillator, and resonance is easy to induce. We can see that the coating layer plays an important role on the resonance and thus on the bandgap. Changing the ratio of the inner and the outer radii is equivalent to changing the properties of the spring, the band structure and gap formation will thus be influenced consequently. We have calculated the gap size and mid-gap frequency at filling fraction 0.204 as a function of the radius ratio. The bars in Figure 2 mark the size of the gap and the line in the middle marks the mid-gap frequencies in the fcc structures. We see the widest gap appears at intermediate radius ratio.

For comparison, in Figure 3 we show the gap width/mid-gap vs. radius ratio for some different filling fractions of the coated spheres. The radius ratio runs from about 0.4 to a limit value. The data label the filling fractions. We can see there is a maximum for each filling fraction. In the filling fraction range discussed, the biggest

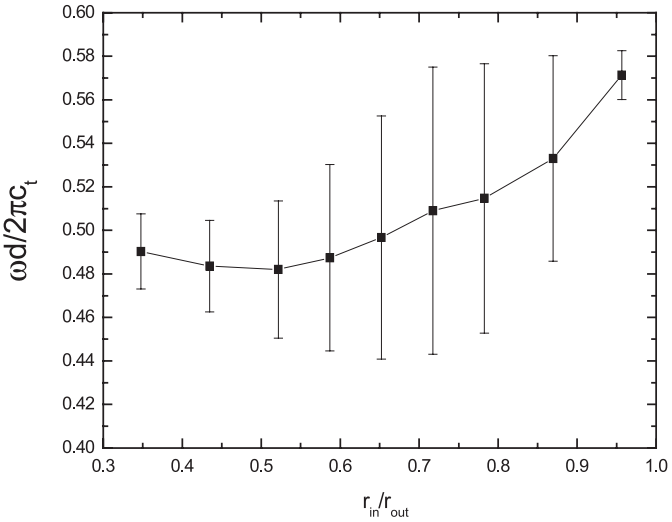

Fig. 2. The gap and the mid-gap frequencies of Au spheres coated by Pb in Si matrix plotted as a function of the ratio of the coating's inner and outer radii. The filling fraction is fixed at 0.204.

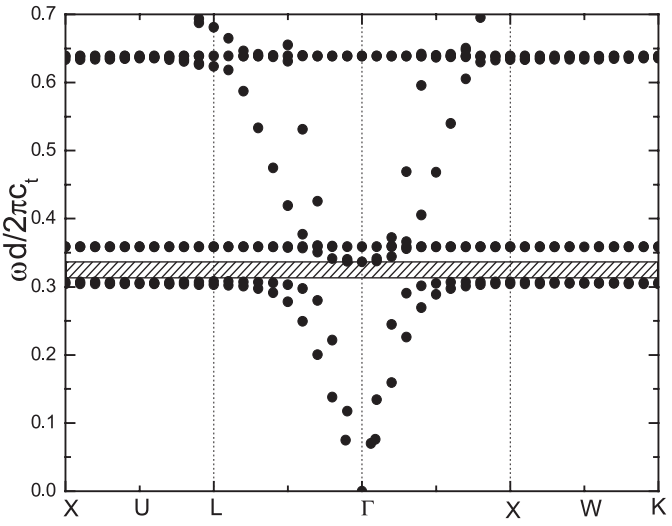

Fig. 4. The elastic wave band structure of Pb spheres coated by plastic embedded in Si matrix arranged in the fcc structure. The filling fraction is 0.204 and the radius ratio r_{in}/r_{out} is 12/23.

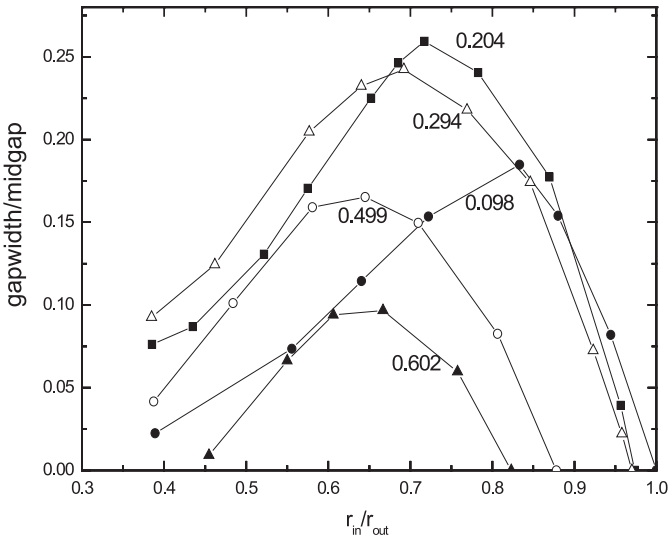

Fig. 3. The gap width/mid-gap vs. the radius ratio for Au-Pb-Si systems with filling fraction at 0.098, 0.204, 0.294, 0.499 and 0.602 respectively.

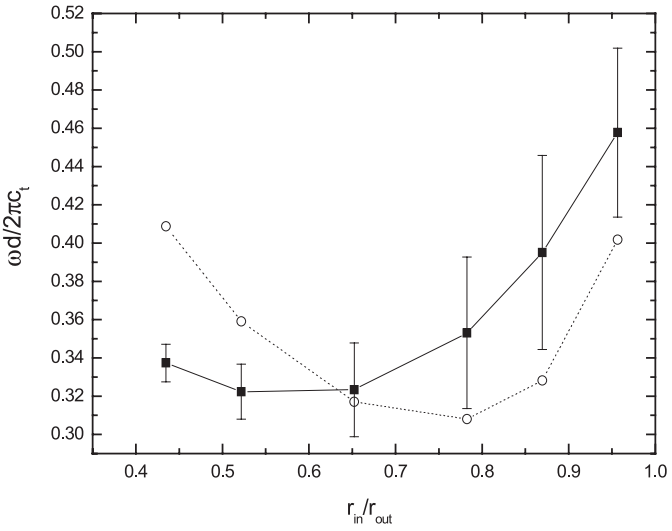

Fig. 5. Solid: the gap and the mid-gap frequencies of Pb spheres coated by plastic embedded in Si matrix. Dotted: the positions of the flat bands, plotted as a function of the radius ratio, the filling fraction is 0.204.

gap appears at filling fraction 0.204 and at radius ratio 0.72. When the radius ratio is further increased, the gaps close gradually. This result is easy to understand as the coating layer gets thinner and thinner till disappearing, the resonance mechanism gradually gets out of its role.

Next, we discuss another three component phononic crystal which is formed by embedding Pb core with plastic coating layer in Si matrix. There is also local resonance in the crystals but in that case the coating layer is even softer relative to the core and the matrix [12]. For this type of system, even at very high filling fraction, the coupling between local units is still rather weak. The local resonance mechanism plays a role in all the filling fraction range, the gap variation with the filling fraction exhibits a completely different behavior at high filling fraction. This is to say, for the second type, it is the pure local resonance mechanism which works across the whole range [12]. The material parameters are chosen as following: $\rho = 11.4$ g/cm^3, $C_l = 2.16$ km/s, $C_t = 0.86$ km/s for Pb; $\rho = 1.19$ g/cm^3, $C_l = 2.75$ km/s, $C_t = 1.2$ km/s for plastic; $\rho = 2.33$ g/cm^3, $C_l = 8.95$ km/s, $C_t = 5.36$ km/s for Si. In Figure 4 we plot the band structure for such a composition with fcc structure and filling fraction 0.204, the radius ratio is again taken 12/23. The lowest gap appears at the frequency of about 0.32, in unit of $d/2\pi C_t$.

We also optimize this gap by tuning the ratio of the coating's inner and outer radii. In Figure 5, we show the

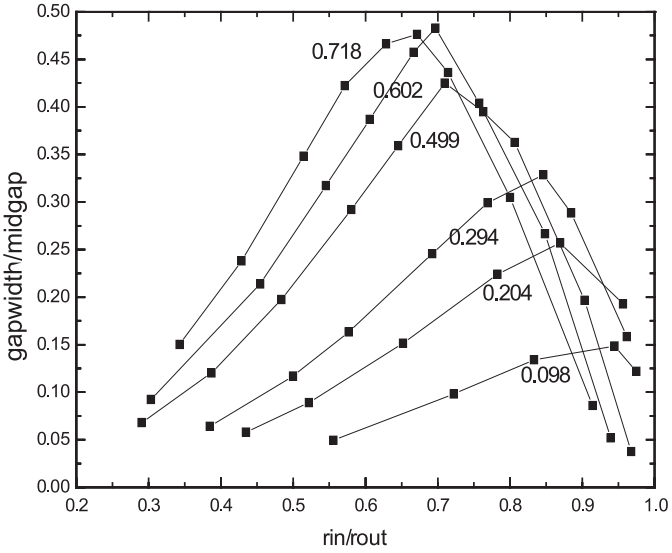

Fig. 6. The gap-width/midgap vs. the radius ratio for Pb-Plastic-Si systems with filling fraction at 0.098, 0.204, 0.294, 0.499, 0.602 and 0.718 respectively.

midgap and gap size (the solid line and the limit), and the flat band (the dotted line) as a function of the radius ratio. Here the filling fraction of the coated spheres is fixed at 0.204. As we expect, the widest gap is found near the radius ratio 0.88 (it is also clearly shown in Fig. 6). For the flat band, when the radius ratio varies from 0.435 to 0.957, it changes from 0.41 to 0.31 and then goes up to 0.4. In the range from 0.585 to 0.76, it appears in the band gap. The flat band corresponds to a shear mode localized in the structural unit, which is a rotational oscillation of the hard sphere around the center. It belongs to each single unit, and is thus dispersiveless in nature. Confined inside the inner core region of the structural unit, it is hard to couple with the external excitations.

In Figure 6, we show the gap width/midgap vs. radius ratio for some different filling fractions. The radius ratio runs from about 0.3 to near a limit value. The data label the filling fractions of coated spheres. We can see there is a maximum for each filling fraction. The radius ratio is smaller than 0.67, the gap width increases with the filling fraction.

This is different from the former case, where the gap width increases to a maximum at an intermediate filling fraction and turns to decrease as the filling fraction increases. It shows that in the present Pb-Plastic-Si system, when the radius ratio is small (which means a relatively thicker coating), the local resonance governs the gap properties. For the former Au-Pb-Si system, the gap narrowing at higher filling fraction is a signature that local resonance mechanism breaks down gradually because of the strong coupling of the resonant units as mentioned above [12]. We can see that although these two systems both fulfill the resonance structure criteria, they show different characters in the gap optimizing process. In the latter system, a pure resonance mechanism dominates even at high filling fraction, which is attributed to the even softer coating layer compared to the former system. It is also interesting to note that for both systems at high radius ratio (which means relatively thin coatings), the gap width decreases monotonically with the filling fraction, which also indicates the failure of the local resonance mechanism because of a short spring that is relatively stiff.

4 Conclusions

In conclusion, we investigate the complete elastic wave band gap in the 3D three-component systems which are based on local resonance. The elastic wave band gap of two systems including Au spheres coated by Pb embedded in a Si matrix and Pb spheres coated by plastic embedded in a Si matrix are discussed, using the multiple-scattering method. We optimize the elastic wave band gap by tuning the ratio of the coating's inner and outer radii. We obtain the optimum gap for the first system at radius ratio of 0.72 and filling fraction of 0.204, and for the second system at radius ratio of 0.70 and filling fraction of 0.602. The optimization of these 3D three-component systems not only serves as an excellent prototype for further understanding the mechanisms leading to classical wave gaps and their interplay, but provides a good guide for their applications.

This work was supported by the National Natural Science Foundation of China under Grant No. 10174054, Doctoral Research Foundation of Ministry of Education of China under Grant No. 20020486013 and Guangdong Provincial Natural Science Foundation of China. NO. 013009.

References

1. E. Yablonovitch, T.J. Gmitter, K.M. Leung, Phys, Rev. Lett. **67**, 2295 (1991)
2. J. Joannopoulos, R.D. Meade, J. Winn, Photonic Crystals (Princeton, 1995)
3. E.M. Econoumou, M. Sigalas, J. Acoust. Soc. Am. **95**, 1734 (1994)
4. M. Kafesaki, E.N. Econoumou, Phys. Rev. B **52**, 13317 (1995)
5. M. Kafesaki, M.M. Sigalas, E.N. Econoumou, Solid State Commun. **96**, 285 (1995)
6. M.S. Kushwaha, B. Djafari-Rouhani, J. Appl. Phys. **80**, 3191 (1996)
7. M.S. Kushwaha, B. Djafari-Rouhani, J. Sound and Vibration **218**, 697 (1998)
8. M.M. Sigalas, J. Acoust. Soc. Am. **101**(3), 1256 (1997)
9. R. Mártinez-Sala, J. Sancho, J.V. Sánchez, V. Gómez, J. Llinares, F. Meseguer, Nature **379**, 241 (1995)
10. Zhengyou Liu, Xixiang Zhang, Yiwei Mao, Y.Y. Zhu, Z. Yang, C.T. Chan, P. Sheng, Science **289**, 1734 (2000)
11. Zhengyou Liu, C.T. Chan, P. Sheng, A.L. Goertzen, J.H. Page, Phys. Rev. B **62**, 2446 (2000)
12. Zhengyou Liu, C.T. Chan, P. Sheng, Phys. Rev. B **65**, 165116 (2002)
13. M.S. Kushwaha, B. Djafari-Rouhani, J. Appl. Phys. **84**, 4677 (1998)

14. M.S. Kushwaha, B. Djafari-Rouhani, L. Dobrzynski, Phys. Lett. A **248**, 252 (1998)
15. M. Kafesaki, R.S. Penciu, E.N. Economou, Phys. Rev. Lett. **84**, 6065 (2000)
16. C. Goffaux, J. Sánchez-Dehesa, A. Levy Yeyati, Ph. Lambin, A. Khelif, J.O. Vasseur, B. Djafari-Rouhani, Phys. Rev. Lett. **88**, 225502 (2002)
17. Xin Zhang, Zhengyou Liu, Youyan Liu, Fugen Wu, Phys. Lett. A **313**, 455 (2003)
18. Xin Zhang, Zhengyou Liu, Jun Mei, Youyan Liu, J. Phys: Condens. Matter **15**, 1 (2003)
19. Fugen Wu, Zhengyou Liu, Youyan Liu, Phys. Rev. E **66**, 046628 (2002)
20. R. Sainidou, N. Stefanou, A. Modinos, Phys. Rev. B **66**, 212301 (2002)
21. J.O. Vasseur, P.A. Deymier, B. Chenni, B. Djafari-Rouhani, L. Dobrzynski, D. Prevost, Phys. Rev. Lett. **86**, 3012 (2001)
22. M. Kafesaki, M.M. Sigalas, N. García, Physica B **296**, 190 (2001)
23. Ph. Lambin, A. Khelif, J.O. Vasseur, L. Dobrzynski, B. Djafari-Rouhani, Phys. Rev. E **63**, 066605 (2001)
24. Y. Tanaka, Y. Tomoyasu, S. Tamura, Phys. Rev. B **60**, 13294 (1999)
25. I.E. Psarobas, N. Stefanou, A. Modinos, Phys. Rev. B **62**, 278 (2000)
26. C. Goffaux, J.P. Vigneron, Phys. Rev. B **64**, 075118 (2001)
27. M. Torres, F.R. Montero de Espinosa, J.L. Aragon, Phys. Rev. Lett. **86**, 4282 (2001)
28. R. Biswas, M.M. Sigalas, K.M. Ho, S.-Y. Lin, Phys. Rev. B **65**, 205121 (2002)
29. J.O. Vasseur, B. Djafari-Rouhani, L. Dobrzynski, M.S. Kushwaha, P. Halevi, J. Phys: Condens. Matter **6**, 8759 (1994)
30. Shu Zhang, Jianchun Cheng, Phys. Rev. B **68**, 245101 (2003)